

## A Comparison of Different Control Laws in Trajectory Control for a Revolute-Jointed Manipulator

Recep BURKAN

*Erciyes University, Kayseri Vocational College, 38039 Kayseri-TURKEY*  
*e-mail: burkanr@erciyes.edu.tr*

İbrahim UZMAY

*Erciyes University, Mechanical Engineering Department, 38039 Kayseri-TURKEY*  
*e-mail: iuzmay@erciyes.edu.tr*

Received 04.07.2002

### Abstract

This study presents a comparison of different control laws for the trajectory control of a revolute-jointed manipulator. For this purpose, adaptive, robust and sliding mode control algorithms are applied to the model system so as to reduce tracking error at each joint. It is assumed that robot parameters are not known exactly and the system includes some uncertainties and disturbances. Computer simulation study of the revolute-jointed manipulators illustrates the effectiveness of different control algorithms in compensating disturbances and uncertainties for tracking different trajectories and, consequently, appropriate control parameters which reduce the tracking error have been determined.

**Key words:** Adaptive control, Robust control, Sliding mode control, Parameter uncertainty, Tracking error.

### Introduction

Since it is difficult to compute or measure the dynamic properties of various objects having geometrical complexity, robots still face uncertainty when addressing parameters describing the relevant characteristics of a grasped load, such as mass moment of inertia or the exact position of centre of the mass being handled. In the presence of parametric uncertainty, to compensate for the disturbing effects of the above factors adaptive control and robust control methods have been used (Spong and Vidyasagar, 1987; Slotine and Li, 1987). Slotine and Li (1987) derived a new adaptive control algorithm which consists of a PD feedback part and a full dynamics feedforward compensation part with unknown manipulator and payload parameters. In another adaptive approach, Slotine and Li (1988) demonstrated that the position and velocity error converge to zero but that Lyapunov stability was not established. Spong *et al.* (1990) proved that an adaptive robot con-

troller is stable in the Lyapunov sense; however, in the proof the feedback gain matrix is assumed to be constant and diagonal. Egeland and Godhavn (1994) assumed that the feedback gain matrix is to be uniformly positive definite, and proved stability in the Lyapunov sense for adaptive robot control.

Sliding mode control is another robot control technique which has many attractive features such as robustness to parameter variations and sensitivity to disturbances. Because of these properties, sliding mode control has applications in robotics (Yeung and Chen, 1988; Bailey and Arapostathis, 1987). Young (1978) and Slotine (1983, 1985) both studied sliding mode control for robot arms. Chen and Xu (1999) presented a sliding mode control law based on the concept of performance robustness and feedback linearisation. The tracking control problem for a robot-conveyor system was studied using the proposed controller.

Spong (1992) proposed a simple robust control law similar to the adaptive control algorithm devel-

oped by Slotine and Li (1987). In this scheme, the approach of Leitman (1981) or of Corless and Leitmann (1981) was used to design a robust controller. To achieve this, the upper bound on the parametric uncertainty should be known first. Yaz (1993) developed a simple robust control law based on Spong (1992) which can guarantee stability under the same set of conditions. Koo and Kim (1994) presented a robust control law for n-link robot manipulators with parametric uncertainty. Using the Lyapunov stability theory, the uniform ultimate boundedness of the tracking error is proved. The basic control structure is similar to that of Spong (1992), but the proposed control approach needs no prior information about the upper bound of uncertainty.

In this paper, in order to investigate the effects of different control techniques such as adaptive, robust and sliding mode controls on trajectory tracking error, a dynamic model for a revolute-jointed manipulator including some parametric uncertainties is developed. The performance of the proposed control methods in tracking different trajectories are determined, and appropriate control parameters for each control rule are defined.

### Adaptive Control Law

In the absence of friction or other disturbances, the dynamic model of an n-link manipulator can be written as

$$M(q)\ddot{q} + C(q,\dot{q})\dot{q} + G(q) = T \quad (1)$$

where  $q$  is the n-dimensional vector of generalised coordinates,  $T$  is the n-dimensional vector of applied torques (or forces),  $M(q)$  is the  $n \times n$  symmetric positive definite inertia matrix,  $C(q,\dot{q})\dot{q}$  is the n-dimensional vectors of centripetal and Coriolis terms and  $G(q)$  is the n-dimensional vector of gravitational terms.

Equation (1) can also be expressed in the following form (Spong and Vidyasagar, 1989)

$$M(q)\ddot{q} + C(q,\dot{q})\dot{q} + G(q) = Y(q, \dot{q}, \ddot{q})\pi = T \quad (2)$$

where  $\pi$  is a constant p-dimensional vector of inertia parameters and  $Y$  is an  $n \times p$  matrix of known functions of the joint position, velocity and acceleration.

Consider the control law

$$T = M(q)a_o + C(q, \dot{q})v_o + G(q) + K_D\sigma \quad (3)$$

with  $K_D$  is a positive definite matrix. The other quantities are given by

$$\begin{aligned} \tilde{q} &= q_d - q; & \dot{\tilde{q}} &= \dot{q}_d - \dot{q}; & a_o &= \ddot{q}_d + \Lambda\dot{\tilde{q}}; \\ v_o &= \dot{q}_d + \Lambda\tilde{q} \end{aligned} \quad (4)$$

where  $\tilde{q}$  is the error between the desired and the actual position,  $\Lambda$  is a positive definite matrix that describes the nonlinear compensation and decoupling terms as a function of the desired velocity and acceleration, as corrected by the current state ( $q$  and  $\dot{q}$ ) of the manipulator. The term  $K_D\sigma$  shows PD action on the error.  $\sigma$  is taken as

$$\sigma = v_o - \dot{q} = \dot{\tilde{q}} + \Lambda\tilde{q} \quad (5)$$

Suppose that the computational model has the same structure as that of the manipulator dynamic model, but its parameters are not known exactly. The control law (3) is then modified to

$$\begin{aligned} T &= \hat{M}(q)a_o + \hat{C}(q, \dot{q})v_o + \hat{G} + K_D\sigma \\ &= Y(q, \dot{q}, v_o, a_o)\hat{\pi} + K_D\sigma \end{aligned} \quad (6)$$

where  $\hat{\pi}$  represents the available estimate on the parameters, and accordingly  $\hat{M}$ ,  $\hat{C}$  and  $\hat{G}$  denote the estimated terms in the dynamic model. Substituting (6) into (2) gives

$$\begin{aligned} M(q)\dot{\sigma} + C(q,\dot{q})\sigma + K_D\sigma &= -\tilde{M}(q)a_o - \tilde{C}(q, \dot{q})v_o - \tilde{G} \\ &= -Y(q, \dot{q}, v_o, a_o)\tilde{\pi} \end{aligned} \quad (7)$$

where  $\tilde{\pi} = \hat{\pi} - \pi$  is the parameter error.

Error quantities concerning system parameters are characterised by;

$$\tilde{M} = \hat{M} - M, \quad \tilde{C} = \hat{C} - C, \quad \tilde{G} = \hat{G} - G \quad (8)$$

The Lyapunov function candidate is defined as

$$V(\sigma, \tilde{q}, \tilde{\pi}) = \frac{1}{2}\sigma^T M(q)\sigma + \frac{1}{2}\tilde{q}^T B\tilde{q} + \frac{1}{2}\tilde{\pi}^T K_\pi\tilde{\pi} > 0 \quad (9)$$

where  $\pi$  is a  $p$ -dimensional vector containing the unknown manipulators and load parameters, and  $\hat{\pi}$  is its estimate, while  $\tilde{\pi} = \hat{\pi} - \pi$  denotes the parameter estimation error vector.  $B$  and  $K_\pi$  are the positive definite usually diagonal matrix. Using the property  $\sigma^T [M(q) - 2C(q, \dot{q})] \sigma = 0 \quad \forall \sigma \in R^n$  and choosing  $B = 2\Lambda K_D$ , the time derivative of  $V(\sigma, \tilde{q}, \tilde{\pi})$  along the trajectory of syssem (7) is

$$\begin{aligned} \dot{V}(\sigma, \tilde{q}, \tilde{\pi}) = & -\dot{\tilde{q}}^T K_D \dot{\tilde{q}} - \tilde{q}^T \Lambda K_D \Lambda \tilde{q} \\ & + \tilde{\pi}^T (K_\pi \dot{\tilde{\pi}} - Y^T(q, \dot{q}, v_0, a_0) \sigma) \end{aligned} \quad (10)$$

If the estimate of the parameter vector is updated as in the adaptive law

$$\dot{\pi} = K_\pi^{-1} Y^T(q, \dot{q}, v_0, a_0) \sigma \quad (11)$$

Eq. (10) becomes

$$\dot{V} = -\dot{\tilde{q}}^T K_D \dot{\tilde{q}} - \tilde{q}^T \Lambda K_D \Lambda \tilde{q} \leq 0 \quad (12)$$

It should be noted that  $\dot{\hat{\pi}} = \dot{\tilde{\pi}}$  ( $\pi$  is constant) (Sciavicco and Siciliano, 1996). The resulting block diagram of adaptive control is illustrated in Figure 1.

### Robust Control Law

Consider the nominal control vector for the model system described by Eqs. (1) and (2).

$$\begin{aligned} T_0 &= M_0(q) a_0 + C_0(q, \dot{q}) v_0 + G_0(q) - K_D \sigma \\ &= Y(q, \dot{q}, v_0, a_0) \pi_0 - K_D \sigma \end{aligned} \quad (13)$$

The nominal control vector  $T_0$  in Eq. (13) is defined in terms of known parameters given by  $\pi_0$ . The other quantities as distinct from adaptive law are given by

$$\begin{aligned} \tilde{q} &= q - q_d \quad \dot{\tilde{q}} = \dot{q} - \dot{q}_d \quad a_0 = \ddot{q}_d - \Lambda \dot{\tilde{q}} \\ v_0 &= \dot{q}_d - \Lambda \tilde{q} \quad \sigma = \dot{\tilde{q}} + \Lambda \tilde{q} \end{aligned} \quad (14)$$

The control input  $T$  can be defined in terms of the nominal control vector  $T_0$

$$T = T_0 + Y(q, \dot{q}, v_0, a_0) \tau = Y(q, \dot{q}, v_0, a_0) (\pi_0 + \tau) - K_D \sigma \quad (15)$$

It is assumed that both  $\pi_0$  and  $\rho$  are known, the parametric uncertainty  $\tilde{\pi}$  is,

$$\|\tilde{\pi}\| = \|\pi - \pi_0\| \leq \rho \quad (16)$$

Let  $\varepsilon > 0$  and choose the additional control vector as defined by Spong (1992) as

$$\tau = \begin{cases} -\rho \frac{Y^T \sigma}{\|Y^T \sigma\|} & \text{if } \|Y^T \sigma\| > \varepsilon \\ -\rho \frac{Y^T \sigma}{\varepsilon} & \text{if } \|Y^T \sigma\| \leq \varepsilon \end{cases} \quad (17)$$

As a measure of parameter uncertainty on which the additional control input is based,  $\rho$  can be defined as

$$\rho = \left( \sum_{i=1}^p p_i^2 \right)^{1/2} \quad (18)$$

The block diagram of robust control is illustrated in Figure 2.

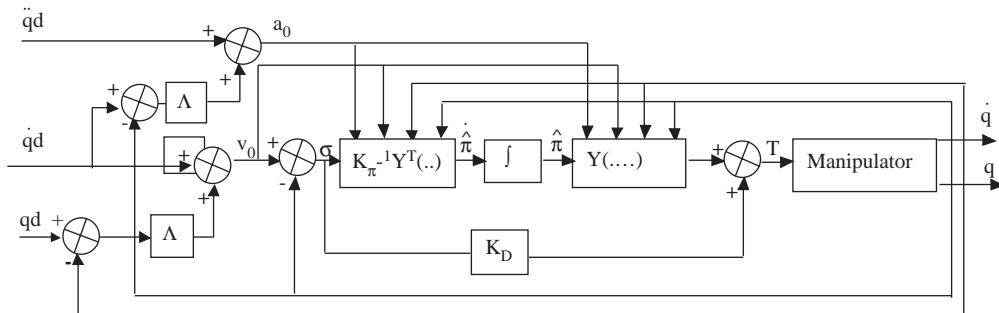
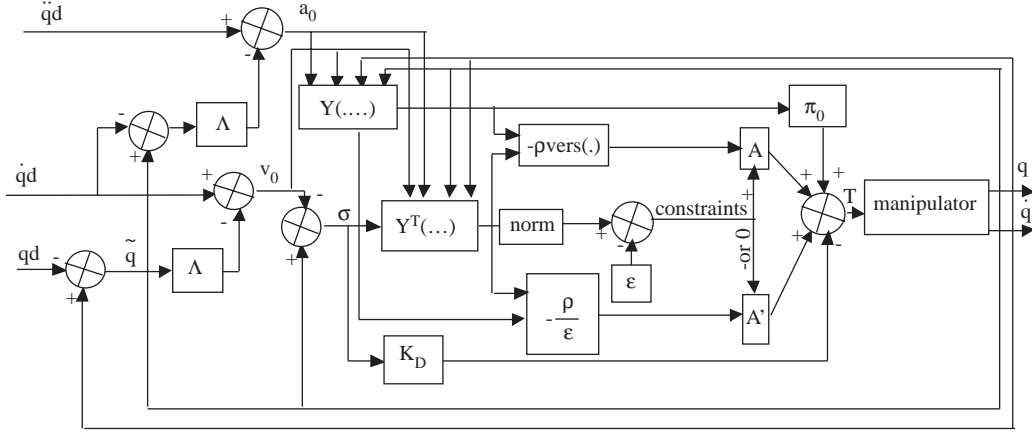


Figure 1. Block diagram of adaptive control (Sciavicco and Siciliano, 1996).



**Figure 2.** Block diagram of the robust control law.

Since the controller defined by Eq. (17) consists of 2 different inputs depending on  $\varepsilon$ , the matrices  $A$  and  $A'$  are introduced to select an appropriate control input. The  $A$  matrix is diagonal with ones and zeros on the diagonal. When  $\|YT\sigma\| - \varepsilon > 0$ , a one is present in  $A$ , a zero is present in  $A'$  and the first additional control input is in effect. When  $\|YT\sigma\| - \varepsilon \leq 0$ , a zero is present in  $A$ , a one is present in  $A'$ , and so the second additional control input is in effect. Hence, the matrices  $A$  and  $A'$  are simple switches which set the mode of additional control input to be used.

If an individual unique bound is assigned for each parameter separately as

$$|\tilde{\pi}_i| \leq \rho_i \quad i = 1, 2, \dots, p \quad (19)$$

Let  $v_i$  denote the  $i$ th component of the vector  $Y^T\sigma$ ,  $\varepsilon_i$  represent the  $i$ th component of  $\varepsilon$ , and define the  $i$ th component of the control input  $\tau_i$  as (Spong, 1992), then

$$\tau = \begin{cases} -\rho_i v_i / |v_i| & \text{if } |v_i| > \varepsilon_i \\ -(\rho_i / \varepsilon_i) v_i & \text{if } |v_i| \leq \varepsilon_i \end{cases} \quad (20)$$

### Sliding Mode Control Law

In order to adapt the computational model to sliding mode control law, the dynamic model of an  $n$ -link manipulator expressed by (1) can be written as

$$M(q)\ddot{q} + h(q, \dot{q}) = T \quad (21)$$

where  $h(q, \dot{q}) = C(q, \dot{q})\dot{q} + G(q)$ .

Since not all parameters of industrial robots are determined correctly,  $M(q)$  and  $h(q, \dot{q})$  are written as

$$M(q) = M^0(q) + \tilde{M}(q), \quad h(q, \dot{q}) = h^0(q, \dot{q}) + \tilde{h}(q, \dot{q}) \quad (22)$$

where “0” denotes the nominal value and “ $\sim$ ” denotes the estimating error. In the sequel, it is assumed that it can be written as

$$|\tilde{M}(q)| \leq (M(q)_{ij})_m, \quad |\tilde{h}(q, \dot{q})| \leq (h_i)_m \quad (23a)$$

where “ $m$ ” denotes the maximal absolute estimating error of each element. At the same time, it is assumed that

$$|\dot{M}_{ij}| \leq \dot{M}_{ij}(q, \dot{q})_m \quad (23b)$$

Finally, it is supposed that the angular acceleration of the desired trajectory  $\ddot{q}_d$  is bounded so that

$$|\tilde{M}(q)\ddot{q}_d| \leq v_i^t(t) \quad (23c)$$

Tracking error is defined as follows:

$$e(t) = q(t) - q_d(t); \quad \dot{e}(t) = \dot{q}(t) - \dot{q}_d(t) \quad (24)$$

where  $q(t)$  and  $\dot{q}(t)$  are assumed to be measurable.

Switching plane is described by

$$s(t) = \Lambda e(t) + \dot{e}(t), \quad \Lambda = \text{diag}(\lambda_1, \lambda_2, \dots, \lambda_2), \quad \lambda_i > 0. \quad (25)$$

Convergence of  $e(t)$  to zero leads to  $s(t) = 0$ . Therefore, the main problem is how to construct the input  $T(t)$  which forces  $s(t)$  to be zero. For this purpose, the following Lyapunov function candidate is introduced.

$$V = (1/2)s^T(t)M(q)s \quad (26)$$

Taking time derivative of (26) and substitute (21), (24) and (25) yields

$$\begin{aligned} \dot{V} &= (1/2)s^T \dot{M}s + s^T M \dot{s} = (1/2)s^T \dot{M}s \\ &\quad + s^T [M\Lambda \dot{e} + M\ddot{q} - M\ddot{q}_d] \\ &= (1/2)s^T \dot{M}s + s^T [M\Lambda \dot{e} - h + T - M\ddot{q}_d] \end{aligned} \quad (27)$$

The control input is introduced as

$$\begin{aligned} T &= -M^0(q)[\Lambda \dot{e}(t) - \ddot{q}_d] + h(q, \dot{q}) \\ &\quad - P(t)s(t) - Q(t)sgn(s) \end{aligned} \quad (28a)$$

where

$$\begin{aligned} Q(t) &= \text{diag}\{q_1(t), \dots, q_n(t)\}, P(t) \\ &= \text{diag}\{p_1(t), \dots, p_n(t)\} \end{aligned} \quad (28b)$$

$Q(t)$  and  $P(t)$  will be determined so that  $\dot{V}$  becomes negative definite using only the upper bound of parameters. The function  $sgn(\cdot)$  is defined as

$$Sgn(s) = +1, \quad s > 0; \quad sgn(s) = -1, \quad s < 0 \quad (29)$$

When  $s$  is a scalar and

$$(1/2) \begin{bmatrix} \sum_{j=1}^n (\dot{M}_{1j})_m - \dot{M}_{11} & -\dot{M}_{12}, \dots, & -\dot{M}_{1n} \\ -\dot{M}_{21} & \sum_{j=1}^n (\dot{M}_{2j})_m - \dot{M}_{22}, \dots & -\dot{M}_{2n} \\ -\dot{M}_{n1}, \dots & -\dot{M}_{n2} & \sum_{j=1}^n (\dot{M}_{nj})_m - \dot{M}_{nn} \end{bmatrix} + \text{diag}(k_1, k_2, \dots, k_n) \quad (35)$$

and the first term of (35) becomes a positive semi-definite matrix from the Gerschgorin theorem. Therefore,  $\dot{V}$  in (31) can be described by

$$\dot{V} \leq -s^T \text{diag}(k_1, k_2, \dots, k_n)s \leq 0 \quad (36)$$

$$Sgn(s) = [sgn(s_1), sgn(s_2), \dots, sgn(s_n)]^T \quad (30)$$

when  $s$  is a vector.

Substituting (22) and (28) into (27) yields

$$\begin{aligned} \dot{V} &= (1/2)s^T \dot{M}s + s^T [M\Lambda \dot{e} - h - M\ddot{q}_d] \\ &\quad + s^T \{ -M^0[\Lambda \dot{e} - \ddot{q}_d] + h^0 - Ps - Qsgn(s) \} \\ &= -s^T [P - \dot{M}/2]s + s^T [ -Qsgn(s) \\ &\quad + \tilde{M}\Lambda \dot{e} - \tilde{h} - \tilde{M}\ddot{q}_d] \end{aligned} \quad (31)$$

Noting that  $sgn(s_i)s_i = |s_i|$  and  $s^T Qsgn(s) = q_1(t)|s_1| + \dots + q_n(t)|s_n|$

Equations (32) and (33) are definite to assure that the second term in (31) is a negative semi-definite function.

$$q_i(t) = \sum_{j=1}^n \{M_m \Lambda\}_{ij} |\dot{e}_j| + (h_i)_m + v_i \quad (32)$$

$$s^T Qsgn(s) \geq s^T (\tilde{M}\dot{e} - \tilde{h} - \tilde{M}\ddot{q}_d) \quad (33)$$

In addition to these, the  $i$ th component of  $P$  in Eq. (31) is defined as

$$p_i(t) = \sum_{j=1}^n (\dot{M}_{ij})_m / 2 + k_i, \quad k_i > 0 \quad (34)$$

Then the  $P - \dot{M}/2$  in the first term of (31) becomes

and it becomes a negative-definite function of  $s$ .

From the Lyapunov second method, from which  $s \rightarrow 0$  is obtained, the sliding mode described by  $s(t) = 0$  occurs provided that the control law (28) with (32) and (34) is used (Chen *et al.*, 1990). The resulting block diagram of sliding mode control is illustrated in Figure 3.

**Robot Parameters and Uncertainty Bounds**

As an illustration, adaptive, robust and sliding mode control algorithms are applied to the revolute-jointed manipulator shown in Figure 4. Robot link parameters are as follows:

$$\begin{aligned} \pi_1 &= I_0, \pi_2 = m_1 l_{c1}^2 + I_1, \pi_3 = m_2 l_1^2, \pi_4 = m_2 l_1 l_{c2}^2, \\ \pi_5 &= m_2 l_{c2}^2 + I_2, \pi_6 = m_1 l_{c1}, \pi_7 = m_2 l_1, \pi_8 = m_2 l_{c2} \end{aligned} \tag{37}$$

For illustrative purposes, let us assume that the parameters of the unloaded manipulator are known, and the chosen values of the link parameters are given by Table 1. Using these values in Table 1, the  $i$ th components of  $\pi$  obtained from Eq. (37) are given in Table 2. These parametric values also show the lower bounds and the unloaded robot parameters.

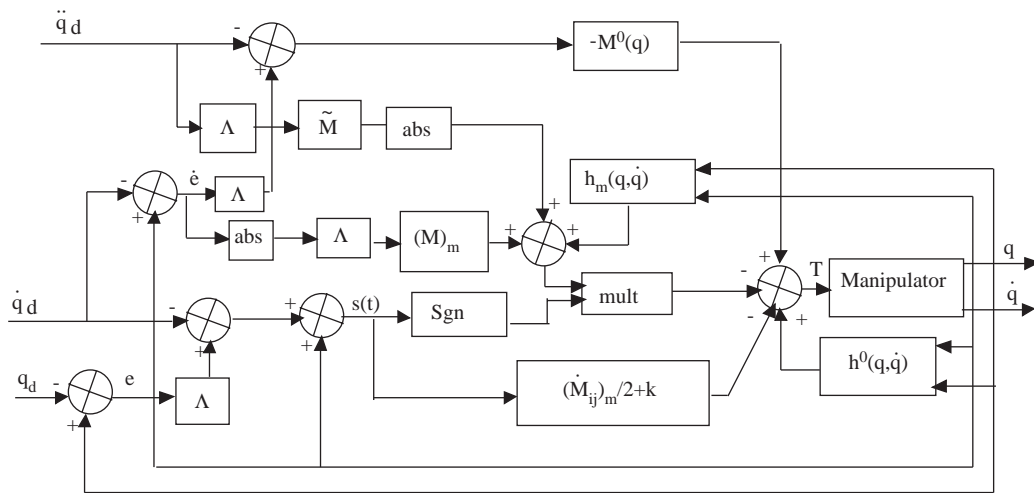


Figure 3. Block diagram of the sliding mode control law.

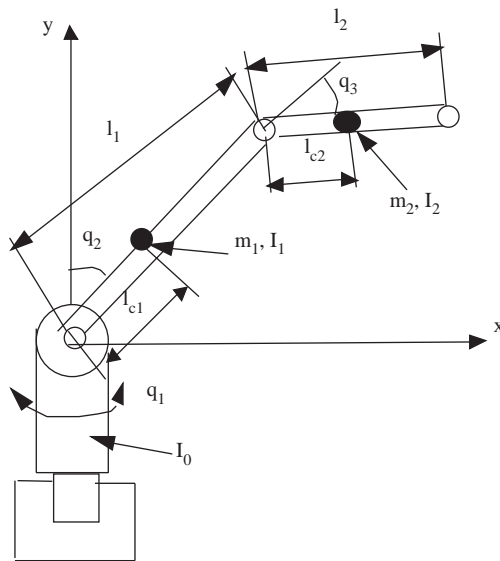


Figure 4. Revolute-jointed manipulator structure (Rivin, 1987).

**Table 1.** Link parameters of the unloaded arm.

$m_1$ (kg)	$m_2$ (kg)	$l_1$ (m)	$l_2$ (m)	$l_{c1}$ (m)	$l_{c2}$ (m)	$I_0$ (kgm <sup>2</sup> )	$I_1$ (kgm <sup>2</sup> )	$I_2$ (kgm <sup>2</sup> )
10	5	1	1	0.5	0.5	3	10/12	5/12

**Table 2.** Inertia values for the unloaded arm.

$\pi_1$	$\pi_2$	$\pi_3$	$\pi_4$	$\pi_5$	$\pi_6$	$\pi_7$	$\pi_9$
3	3.33	5	1.25	1.67	5	5	2.5

If an unknown load carried by the robot is regarded as part of the second link, then the parameters  $m_2$ ,  $l_{c2}$ , and  $I_2$  will change to  $m_2+\Delta m_2$ ,  $l_{c2}+\Delta l_{c2}$  and  $I_2+\Delta I_2$  respectively. The controller is designed to provide robustness in the intervals

$$\begin{aligned} 0 \leq \Delta m_2 \leq 10; \quad 0 \leq \Delta l_{c2} \leq 0.5 \\ 0 \leq \Delta I_2 \leq \frac{15}{12} \end{aligned} \quad (38)$$

$\pi_0$  is chosen as a vector of nominal inertial parameters, and so the loaded arm parameters and their upper bounds are defined. The computed values for the  $i$ th component of  $\pi_0$  are given in Table 3. The difference between the values given in Table 3 and Table 2 are described as the uncertainty bounds  $\rho$ , and the relevant values are given in Table 4.

**Table 3.** Nominal inertia parameter vector,  $\pi_0$ .

$\pi_{01}$	$\pi_{02}$	$\pi_{03}$	$\pi_{04}$	$\pi_{05}$	$\pi_{06}$	$\pi_{07}$	$\pi_{09}$
3	3.33	10	3.9	8.96	5	10	8.75

**Table 4.** Uncertainty bounds.

$\rho_1$	$\rho_2$	$\rho_3$	$\rho_4$	$\rho_5$	$\rho_6$	$\rho_7$	$\rho_9$
0	0	5	2.65	7.29	0	5	6.25

### Conclusion

In the presence of uncertainty, adaptive, robust or sliding mode control laws are used. In the adaptive control strategy, parameters are estimated using an estimation law to control the system properly, and the parameters are assumed to be unknown and bounded. Updating the algorithm stops when it reaches its known bound and resumes updating as soon as a corresponding adaptation algorithm changes sign. In adaptive control law, the parameter adaptation law does not ensure that  $\hat{\pi}$  tends to  $\pi$ ; indeed, the convergence of parameters to their

true values depends on the structure of the matrix  $Y(q, \dot{q}, v_0, a_0)$  and then on the desired and actual trajectories. The term  $Y\hat{\pi}$  ensures an approximate compensation for nonlinear effects,  $K_D\sigma$  introduces a stabilising linear control action of the PD type to the tracking error, and the matrix  $K_\pi$  determines the convergence rate of parameters to their asymptotic values. In robust control, the parameters are not estimated to be distinct from adaptive control, and a control input is defined as a function of fixed nominal parameters and the uncertainty bound. In robust control, the nominal control vector  $T_0$  in Eq. (13) is defined in terms of fixed parameters given by  $\pi_0$ . These parameters are not changed or updated in time as they would be in adaptive control strategy. The additional control input in Eq. (15) is designed to achieve robustness to the parametric uncertainty represented by  $\rho$ . In sliding mode control, the parametric uncertainty range is also fixed.

For a first series of simulations, a straight-line trajectory in space is considered as a reference trajectory. The manipulator has an end-effector initially at location 1, given as  $[p_x(0) \ p_y(0) \ p_z(0)]$  expressed in base coordinates. It moves in  $t_f$  along a straight line in space to the position  $[p_x(t_f) \ p_y(t_f) \ p_z(t_f)]$ . The area of the trapezoid in Figure 5 is equal to the distance  $D$  between the initial and final points, that is

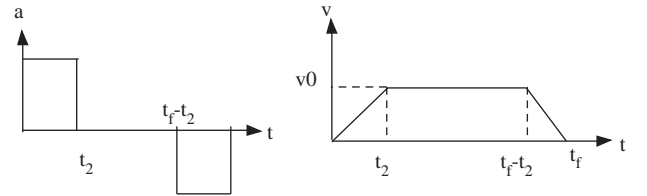


**Figure 5.** Velocity and acceleration profile of the end-effector.

$$D = v_0(t_f - t_2) \quad (39)$$

where  $D = \{(p_x(t_f) - p_x(0))^2 + (p_y(t_f) - p_y(0))^2 + (p_z(t_f) - p_z(0))^2\}^{1/2}$ .

From Figure 5, the following sequence of polynomials is generated to define end-effector positions in space.

$$x(t) = \begin{cases} x_i + \frac{1}{2}at^2 & 0 \leq t \leq t_2 \\ x_i + at_2(t - t_2) & t_2 < t \leq t_f - t_2 \\ x_f - \frac{1}{2}at_2(t_f - t)^2 & t_f - t_2 < t \leq t_f \end{cases} \quad (40)$$

If  $v$  is trajectory velocity, and  $a$  denotes trajectory acceleration of an end effector in space, then the  $x$ ,  $y$  and  $z$  components of velocity ( $v$ ) and acceleration vector ( $a$ ) are defined as

$$\begin{aligned} v_x &= |v| \frac{p_x(t_f) - p_x(0)}{D} & v_y &= |v| \frac{p_y(t_f) - p_y(0)}{D} \\ v_z &= |v| \frac{p_z(t_f) - p_z(0)}{D} \end{aligned} \quad (41)$$

$$\begin{aligned} a_x &= |a| \frac{p_x(t_f) - p_x(0)}{D} & a_y &= |a| \frac{p_y(t_f) - p_y(0)}{D} \\ a_z &= |a| \frac{p_z(t_f) - p_z(0)}{D} \end{aligned} \quad (42)$$

End-effector velocities corresponding to joint velocities are

$$\dot{x} = J(q)\dot{q} \quad (43)$$

Differentiating Eq. (43) yields the acceleration equations

$$\ddot{x} = J(q)\ddot{q} + \left(\frac{d}{dt}J(q)\right)\dot{q} \quad (44)$$

Thus, for a given vector of end-effector accelerations, the instantaneous joint acceleration vector  $\ddot{q}$  is obtained. For this purpose, let

$$b = J(q)\ddot{q} \quad (45)$$

where  $b = \ddot{x} - \frac{d}{dt}J(q)\dot{q}$

If  $\det J(q) \neq 0$ , the inverse velocity and acceleration equations can also be written respectively as (Spong and Vidyasagar, 1989; Koivo 1987)

$$\dot{q} = J(q)^{-1}\dot{x} \quad (46)$$

$$\ddot{q} = J(q)^{-1}b \quad (47)$$

The desired trajectory corresponds to the end-effector position, and so velocity and acceleration are obtained in joint space. The tracking performances obtained using various control techniques are outlined in Figures 6-8 and Tables 5 and 6, respectively. In tracking the given trajectory, the adaptive and robust control laws, which are capable of estimating the parameters and compensating for the uncertainties, provide better results than those of sliding mode control.

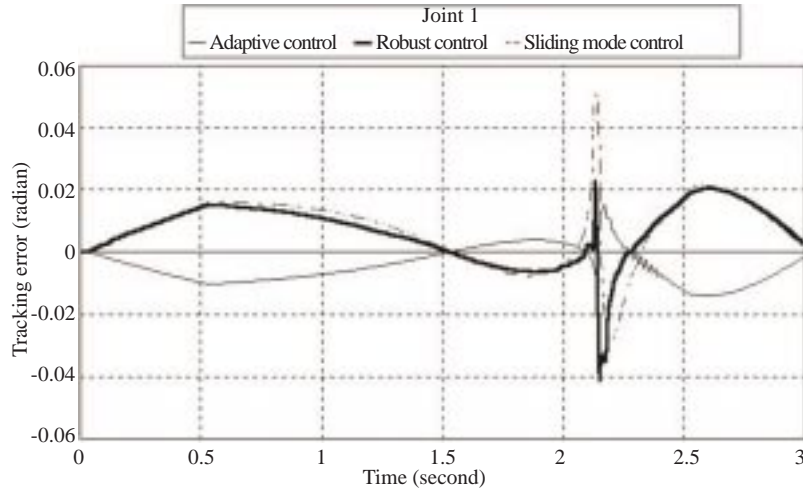


**Figure 6.** Tracking error of joint 1 for straight line trajectory for the adaptive control:  $K_{\pi}^{-1} = \text{diag}[0.2 \ 0.2 \ 0.2 \ 0.2 \ 8 \ 8]$ ,  $\Lambda = \text{diag}[100 \ 100 \ 100]$ ,  $K_D = \text{diag}[600 \ 500 \ 500]$ ; for the robust control:  $\Lambda = \text{diag}[50 \ 50 \ 50]$   $K_D = \text{diag}[500 \ 500 \ 500]$ ,  $\varepsilon = 1$ ; for the sliding mode control:  $\Lambda = \text{diag}[50 \ 50 \ 50]$ ,  $k = \text{diag}[200 \ 200 \ 200]$ .



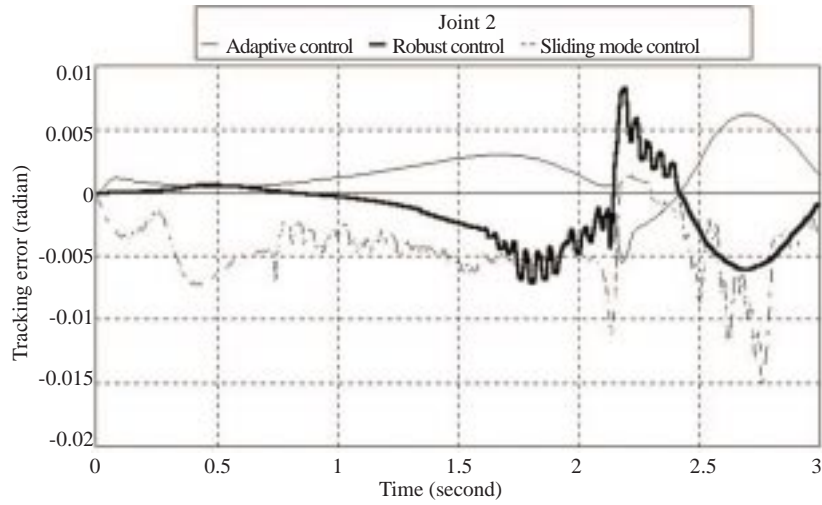


**Figure 7.** Tracking errors of joint 2 for the adaptive control:  $K_{\pi}^{-1} = \text{diag}[0.2 \ 0.2 \ 0.2 \ 0.2 \ 8 \ 8]$ ,  $\Lambda = \text{diag}[100 \ 100 \ 100]$ ,  $K_D = \text{diag}[600 \ 500 \ 500]$ ; for the robust control:  $\Lambda = \text{diag}[50 \ 50 \ 50]$ ,  $K_D = \text{diag}[500 \ 500 \ 500]$ ,  $\varepsilon = 1$ ; for the sliding mode control:  $\Lambda = \text{diag}[50 \ 50 \ 50]$ ,  $k = \text{diag}[200 \ 200 \ 200]$ .

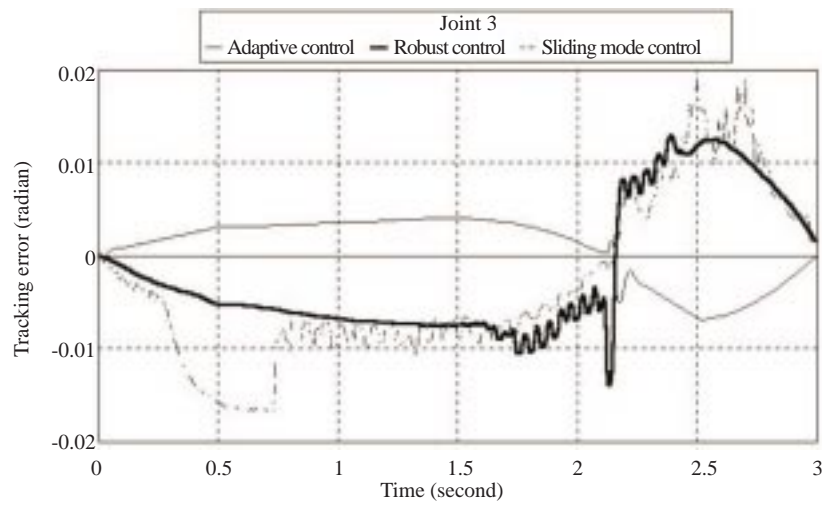


**Figure 8.** Tracking error of joint 3 for the adaptive control:  $K_{\pi}^{-1} = \text{diag}[0.2 \ 0.2 \ 0.2 \ 0.2 \ 8 \ 8]$ ,  $\Lambda = \text{diag}[100 \ 100 \ 100]$ ,  $K_D = \text{diag}[600 \ 500 \ 500]$ ; for the robust control:  $\Lambda = \text{diag}[50 \ 50 \ 50]$ ,  $K_D = \text{diag}[500 \ 500 \ 500]$ ,  $\varepsilon = 1$ ; for the sliding mode control:  $\Lambda = \text{diag}[50 \ 50 \ 50]$ ,  $k = \text{diag}[200 \ 200 \ 200]$ .

**Table 5.** Tracking accuracy in simulation for straight-line trajectory without disturbance.

Tracking error without disturbance at the beginning of motion				Tracking error without disturbance		
Controller	Joint 1	Joint 2	Joint 3	Joint 1	Joint 2	Joint 3
Adaptive control	-0.01	0.0025	0.012	-0.07	0.07	-0.007
Robust control	0.015	-0.0025	-0.042	-0.041	-0.07	-0.014
Sliding mode cont	0.015	-0.007	-0.017	0.05	-0.015	0.02

A second series of simulations was performed with the same trajectory and control parameters with  $\Lambda$ ,  $K_D$  and  $k$  under disturbance torque  $T_d =$

$30[\sin 4\pi; \sin 4\pi; \sin 4\pi]$ . The results are given in Figures 9-11 and Tables 7 and 8. As seen from the relevant graphs and table values, it is clear that the

adaptive controller is capable of compensating for the effect of disturbance. However, in robust and sliding mode controllers, the tracking error has in-

creased at the beginning of the motion. After that point, the tracking error for the sliding mode controller does not change.

**Table 6.** Tracking accuracy in simulation for straight-line trajectory with disturbance

Tracking error with disturbance at the beginning of motion			Tracking error with disturbance			
Controller	Joint 1	Joint 2	Joint 3	Joint 1	Joint 2	Joint 3
Adaptive control	-0.01	0.0025	0.004	-0.017	0.07	-0.007
Robust control	0.015	-0.0025	-0.01	-0.042	0.014	0.016
Sliding mode cont	0.016	-0.009	-0.02	0.05	-0.015	0.02

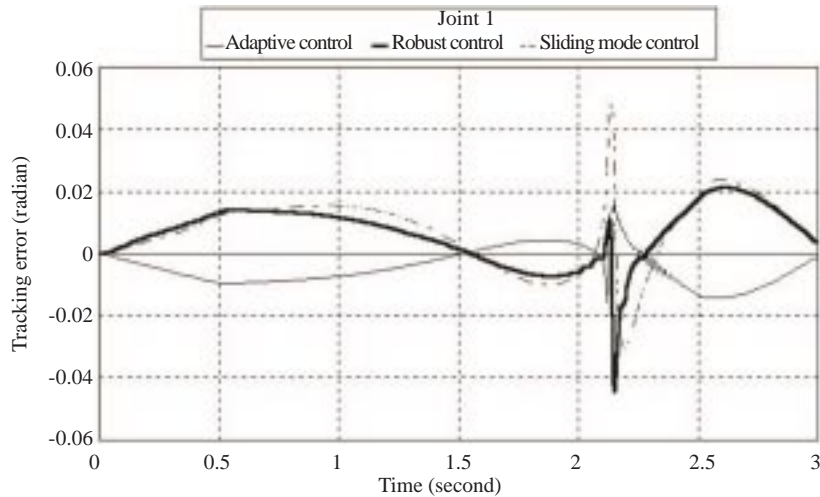


**Figure 9.** Tracking error of joint 1 for the adaptive control:  $K_{\pi}^{-1} = \text{diag}[0.2 \ 0.2 \ 0.2 \ 0.2 \ 8 \ 8]$ ,  $\Lambda = \text{diag}[100 \ 100 \ 100]$ ,  $K_D = \text{diag}[600 \ 500 \ 500]$ ; for the robust control:  $\Lambda = \text{diag}[50 \ 50 \ 50]$ ,  $K_D = \text{diag}[500 \ 500 \ 500]$ ,  $\varepsilon = 1$ ; for the sliding mode control:  $\Lambda = \text{diag}[50 \ 50 \ 50]$ ,  $k = \text{diag}[200 \ 200 \ 200]$ , disturbance  $T_d = 30[\sin 4\pi; \sin 4\pi; \sin 4\pi]$ .

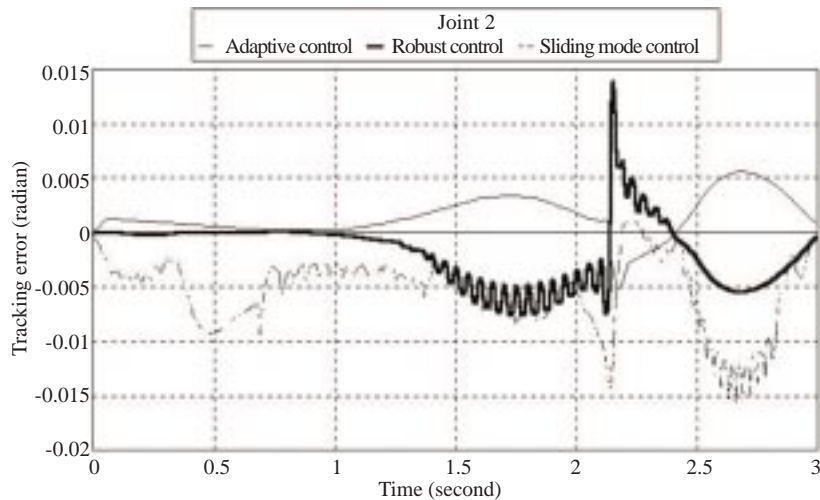


**Figure 10.** Tracking error of joint 2 for adaptive control:  $K_{\pi}^{-1} = \text{diag}[0.2 \ 0.2 \ 0.2 \ 0.2 \ 8 \ 8]$ ,  $\Lambda = \text{diag}[100 \ 100 \ 100]$ ,  $K_D = \text{diag}[600 \ 500 \ 500]$ , for the robust control:  $\Lambda = \text{diag}[50 \ 50 \ 50]$ ,  $K_D = \text{diag}[500 \ 500 \ 500]$ ,  $\varepsilon = 1$ ; for the sliding mode control:  $\Lambda = \text{diag}[50 \ 50 \ 50]$ ,  $k = \text{diag}[200 \ 200 \ 200]$ , the disturbance  $T_d = 30[\sin 4\pi; \sin 4\pi; \sin 4\pi]$ .

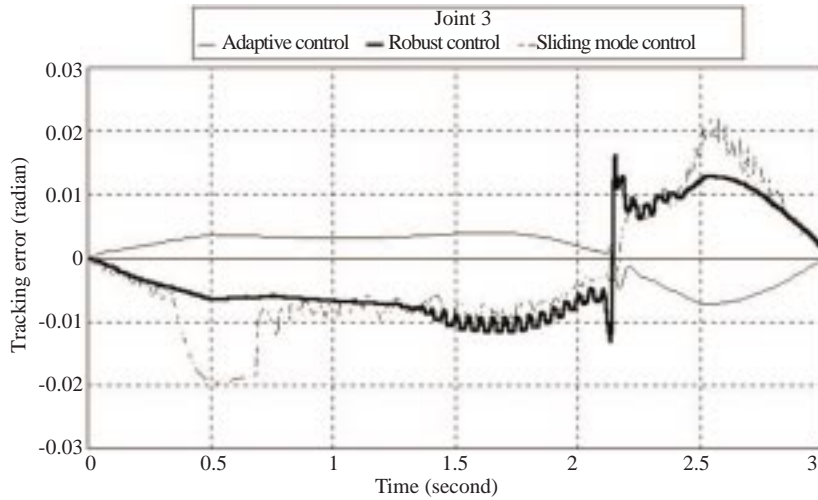


**Figure 11.** Tracking error of joint 3 for the adaptive control:  $K_{\pi}^{-1} = \text{diag}[0.2 \ 0.2 \ 0.2 \ 0.2 \ 8 \ 8]$ ,  $\Lambda = \text{diag}[100 \ 100 \ 100]$ ,  $K_D = \text{diag}[600 \ 500 \ 500]$ ; for the robust control:  $\Lambda = \text{diag}[50 \ 50 \ 50]$ ,  $K_D = \text{diag}[500 \ 500 \ 500]$ ,  $\varepsilon = 1$ ; for the sliding mode control:  $\Lambda = \text{diag}[50 \ 50 \ 50]$ ,  $k = \text{diag}[200 \ 200 \ 200]$ , the disturbance  $T_d = 30[\sin 4\pi; \sin 4\pi; \sin 4\pi]$ .

**Table 7.** Tracking accuracy in simulation for the second trajectory without disturbance.

Tracking error with disturbance at the beginning of motion				Tracking error with disturbance		
Controller	Joint 1	Joint 2	Joint 3	Joint 1	Joint 2	Joint 3
Adaptive control	0.0002	0.0009	0.00025	0.0001	0.0002	0.0002
Robust control	-0.0002	0.0002	0.00001	-0.00025	-0.0003	0.000025
Sliding mode cont	-0.0004	-0.0032	-0.0013	0.00015	-0.003	-0.0004

**Table 8.** Tracking accuracy in simulation for the second trajectory with disturbance.

Tracking error without disturbance at the beginning of motion				Tracking error without disturbance		
Controller	Joint 1	Joint 2	Joint 3	Joint 1	Joint 2	Joint 3
Adaptive control	0.0006	0.001	0.0005	0.0005	-0.0005	0.005
Robust control	-0.0005	-0.0005	-0.0009	-0.0005	-0.0008	-0.009
Sliding mode cont	0.0015	-0.006	-0.0027	-0.0013	-0.004	-0.0027

In order to investigate the performance of the controllers for a given trajectory, a point-to-point motion is considered. It is assumed that the end effector moves from location 1 to location 2 as defined for the previous trajectory and in the second set of simulations, the reference trajectory for each joint is defined as follows:

$$q_d = q_0 + b(t - (1/a)\sin(at)) , \quad \dot{q}_d = b(1 - \cos(at)) \quad (48)$$

The initial and final values of each joint position is calculated according to the first and second locations of the end-effector; it is known that the initial and final values of the joint velocity and acceleration

should be zero. Operation time is chosen to be 3 s. By taking these conditions, the parameters ( $a$ ) and ( $b$ ) can be computed.

The tracking responses of the adaptive, robust and sliding mode controllers are given in Figures 12-14. The tracking performance of the adaptive controller is poor but the robust controller is better with control parameters such as  $\Lambda = \text{diag}(150 \ 15 \ 15)$  and  $K_D = \text{diag}(50 \ 50 \ 50)$ . For the robust controller, it is also possible to increase the tracking performance by increasing the control parameters  $\Lambda$  and  $K_D$ . Under the noise signal, the results are outlined in Figures 15-17. The adaptive controller does not suffer from the disturbance but robust and sliding mode controllers are poor in tracking performance.

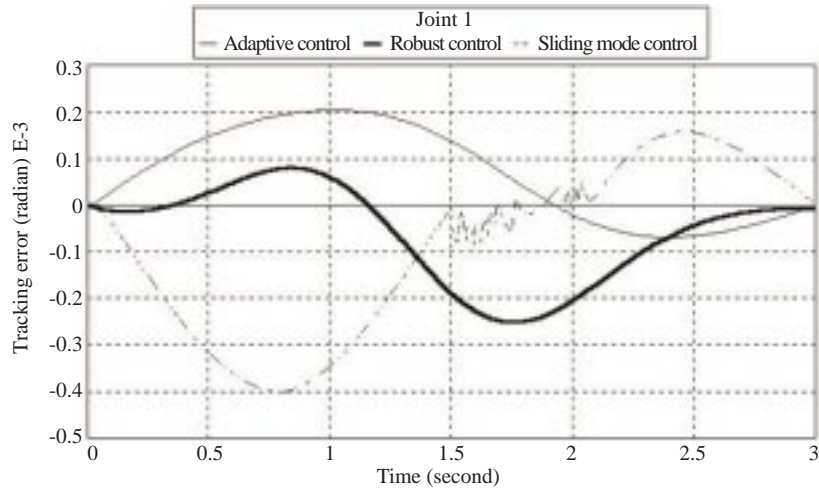


**Figure 12.** Tracking error of joint 1 for second trajectory for the adaptive control:  $K_{\pi}^{-1} = \text{diag}[0.2 \ 0.2 \ 0.2 \ 0.2 \ 8 \ 8]$ ,  $\Lambda = \text{diag}[100 \ 100 \ 100]$ ,  $K_D = \text{diag}[600 \ 700 \ 700]$ ; for the robust control:  $\Lambda = \text{diag}[150 \ 15 \ 15]$ ,  $K_D = \text{diag}[50 \ 50 \ 50]$ ,  $\varepsilon = 1$ ; for the sliding mode control:  $\Lambda = \text{diag}[100 \ 50 \ 50]$ ,  $k = \text{diag}[250 \ 250 \ 250]$ .

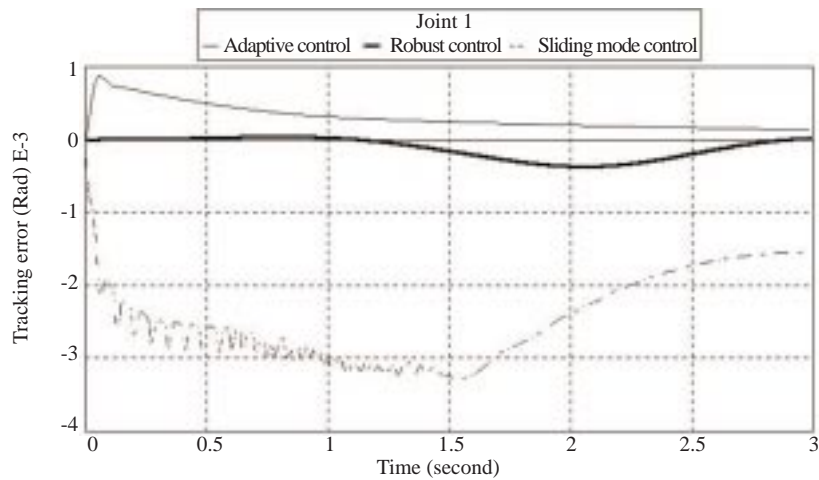


**Figure 13.** Tracking error of joint 2 for second trajectory for the adaptive control:  $K_{\pi}^{-1} = \text{diag}[0.2 \ 0.2 \ 0.2 \ 0.2 \ 8 \ 8]$ ,  $\Lambda = \text{diag}[100 \ 100 \ 100]$ ,  $K_D = \text{diag}[600 \ 700 \ 700]$ ; for the robust control:  $\Lambda = \text{diag}[150 \ 15 \ 15]$ ,  $K_D = \text{diag}[50 \ 50 \ 50]$ ,  $\varepsilon = 1$ ; for the sliding mode control:  $\Lambda = \text{diag}[100 \ 50 \ 50]$ ,  $k = \text{diag}[250 \ 250 \ 250]$ .

In this work, the revolute-jointed manipulator shown in Figure 4 was considered to illustrate the tracking performances of three different controllers for various trajectories, and the efficiency and deficiency of each control scheme under uncertainty and disturbance were analysed. For that purpose, the control parameters were chosen as high as possible, and the parameters were varied until the best performance was obtained in each case. For the straight-line trajectory, the best performance is obtained for an adaptive controller for  $\Lambda \leq 100$ , and for  $K_D$  in the interval  $100 \leq K_D \leq 600$ . If  $K_D$  is larger than

600, then the deviation of actual trajectory from the desired trajectory is very large. These intervals are determined for the robust controller approximately as  $\Lambda \leq 50$  and  $100 \leq K_D \leq 500$ ; for the sliding mode controller for  $50 \leq k \leq 200$  and the tracking performances are changed in these intervals. For the second trajectory, the best performance is obtained for the adaptive controller for  $\Lambda \leq 100$ , and for  $K_D$  in the interval  $100 \leq K_D \leq 700$ , for the robust controller approximately for  $\Lambda \leq 50$  and for  $K_D$ ,  $100 \leq K_D \leq 600$ ; for the sliding mode controller for  $\Lambda < 50$  and  $50 \leq k \leq 250$

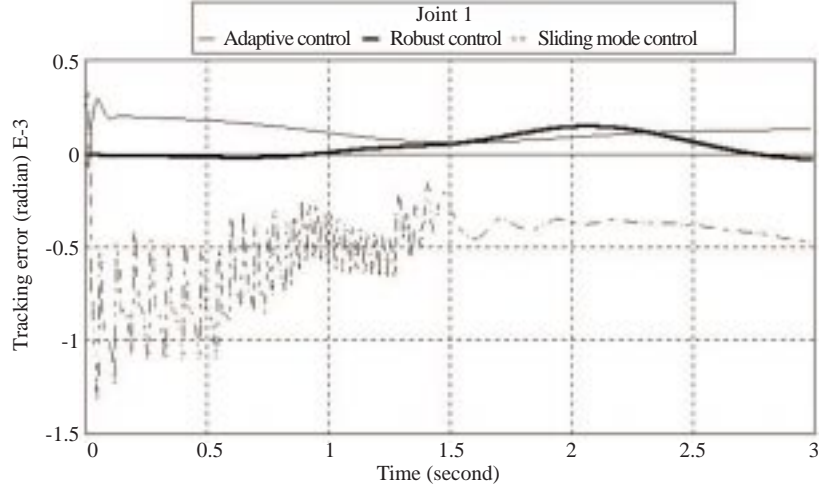


**Figure 14.** Tracking error of joint 3 for second trajectory for the adaptive control:  $K_{\pi}^{-1} = \text{diag}[0.2 \ 0.2 \ 0.2 \ 0.2 \ 8 \ 8]$ ,  $\Lambda = \text{diag}[100 \ 100 \ 100]$ ,  $K_D = \text{diag}[600 \ 700 \ 700]$ ; for the robust control:  $\Lambda = \text{diag}[150 \ 15 \ 15]$ ,  $K_D = \text{diag}[50 \ 50 \ 50]$ ,  $\varepsilon = 1$ ; for the sliding mode control:  $\Lambda = \text{diag}[100 \ 50 \ 50]$ ,  $k = \text{diag}[250 \ 250 \ 250]$ .

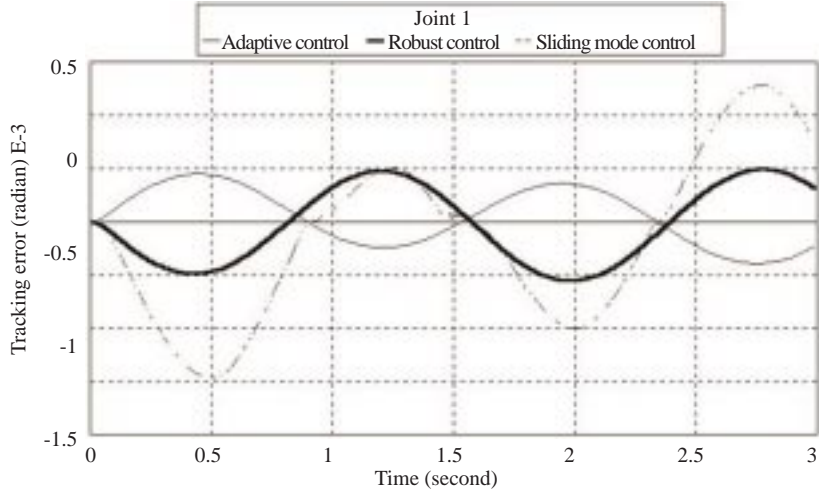


**Figure 15.** Tracking error of the joint 1 for second trajectory and the adaptive control:  $K_{\pi}^{-1} = \text{diag}[0.2 \ 0.2 \ 0.2 \ 0.2 \ 8 \ 8]$ ,  $\Lambda = \text{diag}[100 \ 100 \ 100]$ ,  $K_D = \text{diag}[600 \ 700 \ 700]$ , for the robust control:  $\Lambda = \text{diag}[100 \ 50 \ 50]$ ,  $K_D = \text{diag}[600 \ 600 \ 600]$ ,  $\varepsilon = 1$ ; for the sliding mode control:  $\Lambda = \text{diag}[100 \ 50 \ 50]$ ,  $k = \text{diag}[250 \ 400 \ 250]$ , the disturbance  $T_d = 30[\sin 4\pi; \sin 4\pi; \sin 4\pi]$ .

For the straight-line trajectory the performance of the adaptive controller is better than the others, but for the second trajectory the performance of the adaptive controller is poor. In the straight-line trajectory the joint variables are not smooth that is, there is sudden change in joint velocity and acceleration.

If any deviation of actual trajectory from the desired motion occurs, the adaptation mechanism will tune the estimate  $\hat{\pi}$  and joint torque. Updating the algorithm stops when it reaches its known bound and updating is resumed as soon as the correspond-

ing adaptation algorithms change signs. If there is any sudden change in the joint trajectory orientation or the system faces any disturbance, the actual trajectory will be deviated from the desired path, and the updating algorithm will tune the estimate  $\hat{\pi}$  and the joint torques. Therefore, uncertainty and disturbance will be rejected. If a joint trajectory is smooth, the tracking error will converge to zero then  $Y^T \sigma$  also will converge to zero, so the parameter estimation speed will decrease and exact parameter convergence cannot be achieved. Therefore, the tracking

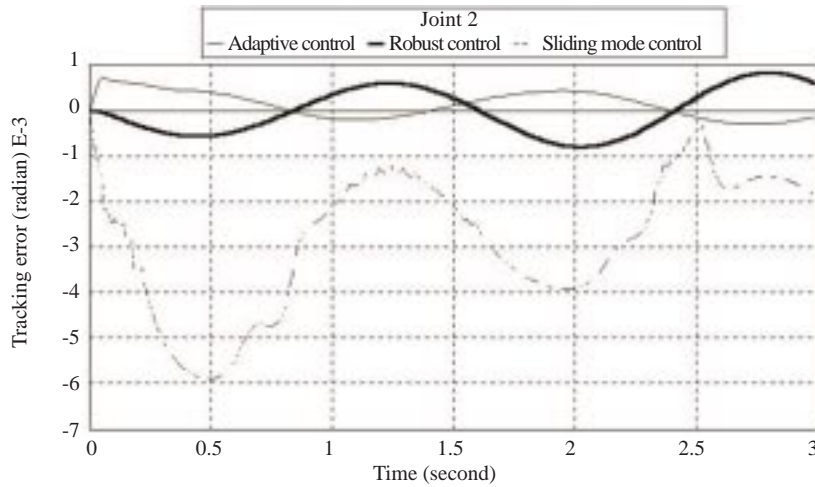


**Figure 16.** Tracking error of joint 2 for second trajectory and the adaptive control:  $K_{\pi}^{-1} = \text{diag}[0.2 \ 0.2 \ 0.2 \ 0.2 \ 8 \ 8]$ ,  $\Lambda = \text{diag}[100 \ 100 \ 100]$ ,  $K_D = \text{diag}[600 \ 700 \ 700]$ ; for the robust control:  $\Lambda = \text{diag}[100 \ 50 \ 50]$ ,  $K_D = \text{diag}[600 \ 600 \ 600]$ ,  $\varepsilon = 1$ ; for the sliding mode control:  $\Lambda = \text{diag}[100 \ 50 \ 50]$ ,  $k = \text{diag}[250 \ 400 \ 250]$ , the disturbance  $T_d = 30[\sin 4\pi; \sin 4\pi; \sin 4\pi]$ .

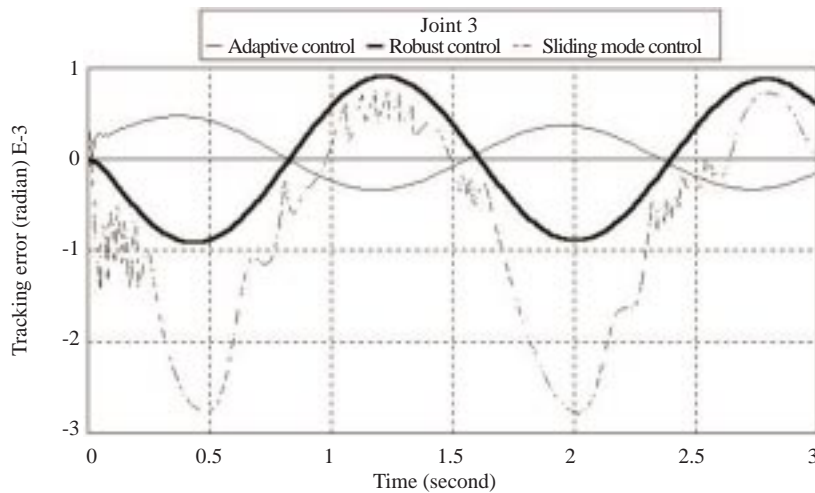


**Figure 17.** Tracking error of joint 3 for second trajectory for the adaptive control:  $K_{\pi}^{-1} = \text{diag}[0.2 \ 0.2 \ 0.2 \ 0.2 \ 8 \ 8]$ ,  $\Lambda = \text{diag}[100 \ 100 \ 100]$ ,  $K_D = \text{diag}[600 \ 700 \ 700]$ ; for the robust control:  $\Lambda = \text{diag}[100 \ 50 \ 50]$ ,  $K_D = \text{diag}[600 \ 600 \ 600]$ ,  $\varepsilon = 1$ ; for the sliding mode control:  $\Lambda = \text{diag}[100 \ 50 \ 50]$ ,  $k = \text{diag}[250 \ 400 \ 250]$ , the disturbance  $T_d = 30[\sin 4\pi; \sin 4\pi; \sin 4\pi]$ .

error will increase. In the case of robust and sliding mode control applications, although the parameters are not changed or updated as they would be in the adaptive control strategy, the additional control input is designed to achieve robustness to the parametric uncertainty.

The question of whether to use robust or adaptive control does not have an obvious answer. If the uncertainty is large and has a computational model, adaptive control is better. In the presence of external disturbances and unmodelled dynamics such as

structural flexibility (Ghorbel, *et al.* 1990), unless the algorithm is modified the performance of adaptive control is poor (Spong, 1992). The robust control algorithm is also simple but suffers from uncertainty if uncertainty is large and chattering happens. However, the robust control law is simpler in design than previous robust algorithms, and if the uncertainty is not large, it may be an alternative to adaptive control (Spong, 1992). As shown in Figures 6-11, the adaptive controller has the best final tracking accuracy and the best tracking performance, and does

not suffer from uncertainty and disturbance as much as robust and adaptive control laws if trajectory is defined in task space. Adaptive control also guarantees trajectory tracking without chattering, and it is simpler than the sliding mode control algorithm. The sliding mode controller has little advantage over adaptive and robust control in the presence of large uncertainty. Since  $\dot{M}(q)$  is required in the case of sliding mode control, it is also not as simple as adaptive and robust control laws.

The performance of the controllers also varies according to trajectory features and disturbances. If a joint trajectory is not smooth and the system faces a disturbance, the performance of the adaptive controller is better. If there is no disturbance and the trajectory is smooth, the robust controller should be preferred. The performance of the sliding mode controller is poor when compared to the adaptive and robust controllers, but it rejects disturbance in the final motion.

## APPENDIX

Applied torque expressions (Rivin, 1987) and dynamic model components.

$$\begin{aligned} T_1 = & \{I_0 + (m_1 l_{c1}^2 + I_1) \cos^2 q_2 + m_2 l_1 [l_1 \cos q_2 + 2l_{c2} \cos(q_2 + q_3) \cos q_2] \\ & + (m_2 l_{c2}^2 + I_2) \cos(q_2 + q_3)\} \ddot{q}_1 + 2\{m_1 l_{c1}^2 + I_1\} \sin q_2 \cos q_3 + m_2 l_1 [l_1 \sin q_2 \cos q_2 \\ & + l_{c2} \sin q_2 \cos(q_2 + q_3)] + (m_2 l_{c2}^2 + I_2) \sin(q_2 + q_3) \cos(q_2 + q_3)\} \dot{q}_1 \dot{q}_2 \\ & + 2[m_2 l_1 l_{c2} \cos q_2 \sin(q_2 + q_3) + (m_2 l_{c2}^2 + I_2) \sin(q_2 + q_3) \cos(q_2 + q_3)] \dot{q}_1 \dot{q}_3 \end{aligned}$$

$$\begin{aligned} T_2 = & (m_1 l_{c1}^2 + I_1 + m_2 l_1^2 + 2m_2 l_1 l_{c2} \cos q_3 + m_2 l_{c2}^2 + I_2) \ddot{q}_2 + m_2 l_1 l_{c2} \cos q_3 + m_2 l_{c2}^2 + I_2) \ddot{q}_3 \\ & - \{(m_1 l_{c1}^2 + I_1) \sin q_2 \cos q_2 + m_2 [l_1^2 \sin q_2 \cos q_2 + l_1 l_{c2} \sin q_2 \cos(q_2 + q_3) \\ & + l_{c2}^2 \sin(q_2 + q_3) \cos(q_2 + q_3)] + I_2 \sin(q_2 + q_3) \cos(q_2 + q_3)\} \dot{q}_1^2 + m_2 l_1 l_{c2} \sin q_3 \dot{q}_2^2 \\ & + 2m_2 l_1 l_{c2} \sin q_3 \dot{q}_2 \dot{q}_3 + g\{m_1 l_{c1} \cos q_2 + m_2 [l_1 \cos q_2 + l_{c2} \cos(q_2 + q_3)]\} \end{aligned}$$

$$\begin{aligned} T_3 = & (m_2 l_1 l_{c2} \cos q_3 + m_2 l_{c2}^2 + I_2) \ddot{q}_2 + (m_2 l_{c2}^2 + I_2) \ddot{q}_3 - \{m_2 [l_1 l_{c2} \cos q_2 \sin(q_2 + q_3) \\ & + l_{c2}^2 \sin(q_2 + q_3) \cos(q_2 + q_3)] + I_2 \sin(q_2 + q_3) \cos(q_2 + q_3)\} \dot{q}_1^2 - (m_2 l_1 l_{c2} \sin q_3) \dot{q}_2^2 \\ & + g[m_2 l_{c2} \cos(q_2 + q_3)] \end{aligned}$$

$$M(q) = \begin{bmatrix} \pi_1 + \pi_2 c_2^2 + \pi_3 c_2 + 2\pi_4 c_{23} c_2 + \pi_5 c_{23} & 0 & 0 \\ 0 & \pi_2 + \pi_3 + 2\pi_4 c_3 + \pi_5 & \pi_4 c_3 + \pi_5 \\ 0 & \pi_4 c_3 + \pi_5 & \pi_5 \end{bmatrix}$$

$$C(q, \dot{q}) = \begin{bmatrix} 2\pi_5 s_{23} c_{23} (\dot{q}_2 + \dot{q}_3) & (2\pi_2 s_2 c_2 + 2\pi_3 s_2 c_2 + 2\pi_4 s_2 c_{23}) \dot{q}_1 & (2\pi_4 c_2 s_{23}) \dot{q}_1 \\ -(\pi_2 s_2 c_2 + \pi_3 s_2 c_2 + \pi_4 s_2 c_{23} + \pi_5 s_{23} c_{23}) \dot{q}_1 & 2\pi_4 s_3 \dot{q}_3 & \pi_4 s_3 \dot{q}_3 \\ -(\pi_4 c_2 s_{23} + \pi_5 s_{23} c_{23}) \dot{q}_1 & -\pi_4 s_3 \dot{q}_2 & 0 \end{bmatrix}$$

$$G(q) = \begin{bmatrix} 0 \\ g\pi_6 c_2 + g\pi_7 c_2 + g\pi_8 c_{23} \\ g\pi_8 c_{23} \end{bmatrix}$$

The components of  $Y(q, \dot{q}, \ddot{q})$ :

$$\begin{aligned}
 y(1, 1) &= \ddot{q}_1; y(1, 2) = \cos(q_2)^2 \ddot{q}_1 + 2\sin(q_2)\cos(q_2)\dot{q}_1\dot{q}_2; y(1, 3) = \cos(q_2)\dot{q}_1 + 2\sin(q_2)\cos(q_2)\dot{q}_1\dot{q}_2 \\
 y(1, 4) &= 2\cos(q_2 + q_3)\cos(q_2)\ddot{q}_1 + 2\cos(q_2)\sin(q_2 + q_3)\dot{q}_1\dot{q}_3 + 2\sin(q_2)\cos(q_2 + q_3)\dot{q}_1\dot{q}_2 \\
 y(1, 5) &= \cos(q_2 + q_3)\dot{q}_1 + 2\sin(q_2 + q_3)\cos(q_2 + q_3)(\dot{q}_1\dot{q}_2 + \dot{q}_1\dot{q}_3) \\
 y(1, 6) &= 0; y(1, 7) = 0; y(1, 8) = 0; y(2, 1) = 0; y(2, 2) = \ddot{q}_3 - \sin(q_2)\cos(q_2)\dot{q}_1^2 \\
 y(2, 3) &= \ddot{q}_3 - \sin(q_2)\cos(q_2)\dot{q}_1^2 \\
 y(2, 4) &= \ddot{q}_3\cos(q_3) + 2\cos(q_3)\ddot{q}_2 - \sin(q_2)\cos(q_2 + q_3)\dot{q}_1^2 + \sin(q_3)\dot{q}_3^2 + 2\sin(q_3)\dot{q}_2\dot{q}_3 \\
 y(2, 5) &= \ddot{q}_2 + \ddot{q}_3 - \sin(q_2 + q_3)\cos(q_2 + q_3)\dot{q}_1^2; y(2, 6) = g\cos(q_2); y(2, 7) = y(2, 6); y(2, 8) = g\cos(q_2 + q_3); \\
 y(3, 1) &= 0; y(3, 2) = 0; y(3, 3) = 0; \\
 y(3, 4) &= \cos(q_3)\ddot{q}_2 - \cos(q_2)\sin(q_2 + q_3)\dot{q}_1^2 - \sin(q_3)\dot{q}_2^2; y(3, 5) = \ddot{q}_3 + \ddot{q}_2 - \sin(q_2 + q_3)\cos(q_2 + q_3)\dot{q}_1^2 \\
 y(3, 6) &= 0; y(3, 7) = 0; y(3, 8) = y(2, 8);
 \end{aligned}$$

The components of  $Y(q, \dot{q}, v_0, a_0)$ :

$$\begin{aligned}
 y0(1, 1) &= a_{01}; y0(1, 2) = \cos(q_2)^2 a_{01} + 2\sin(q_2)\cos(q_2)\dot{q}_1 v_{02}; \\
 y0(1, 3) &= \cos(q_2)a_{01} + 2\sin(q_2)\cos(q_2)\dot{q}_1 v_{02} \\
 y0(1, 4) &= 2\cos(q_2 + q_3)\cos(q_2)a_{01} + 2\cos(q_2)\sin(q_2 + q_3)\dot{q}_1 v_{03} + 2\sin(q_2)\cos(q_2 + q_3)\dot{q}_1 v_{02} \\
 y0(1, 5) &= \cos(q_2 + q_3)a_{01} + 2\sin(q_2 + q_3)\cos(q_2 + q_3)(\dot{q}_2 v_{01} + v_{01}\dot{q}_3) \\
 y0(1, 6) &= 0; y0(1, 7) = 0; y0(1, 8) = 0; \\
 y0(2, 1) &= 0; y0(2, 2) = a_{02} - \sin(q_2)\cos(q_2)\dot{q}_1 v_{01}; y0(2, 3) = a_{02} - \sin(q_2)\cos(q_2)\dot{q}_1 v_{01} \\
 y0(2, 4) &= a_{03}\cos(q_3) + 2\cos(q_3)a_{02} - \sin(q_2)\cos(q_2 + q_3)\dot{q}_1 v_{01} + \sin(q_3)\dot{q}_3 v_{03} + 2\sin(q_3)\dot{q}_3 v_{02} \\
 y0(2, 5) &= a_{02} + a_{03} - \sin(q_2 + q_3)\cos(q_2 + q_3)\dot{q}_1 v_{01} \\
 y0(2, 6) &= g\cos(q_2); y0(2, 7) = y0(2, 6); y0(2, 8) = g\cos(q_2 + q_3); \\
 y0(3, 1) &= 0; y0(3, 2) = 0; y0(3, 3) = 0; y0(3, 4) = \cos(q_3)a_{02} - \cos(q_2)\sin(q_2 + q_3)\dot{q}_1 v_{01} - \sin(q_3)\dot{q}_2 v_{02} \\
 y0(3, 5) &= a_{03} + a_{02} - \sin(q_2 + q_3)\cos(q_2 + q_3)\dot{q}_1 v_{01}; y0(3, 6) = 0; y0(3, 7) = 0; y0(3, 8) = y0(2, 8);
 \end{aligned}$$

**Nomenclature**

		$q_d$	the vector of desired position
A and $A'$	diagonal matrices with ones and zeros on the diagonal	$\tilde{q}, \dot{\tilde{q}}$	position and velocity errors
$e(t)$	tracking error	$s(t)$	switching plane
K, $\Lambda$ , B and $K_\pi$	positive definite, usually diagonal matrices	V	Lyapunov function candidate
$K\sigma$	a vector of PD action	$Y(q, \dot{q}, \ddot{q})$	a matrix which is a function of joint positions, velocities and accelerations
$M(q), C(q, \dot{q})$	inertia matrix, centripetal/coriolis and gravitational vectors	$\hat{\pi}$	estimate of the available parameters
$\dot{q}$ and $G(q)$		$\tilde{\pi}$	parameter error vector
$\hat{M}, \hat{C}$ and $\hat{G}$	estimated terms in the dynamic model	$\pi_0$	a vector of nominal loaded arm parameters and their upper bounds
$q, \dot{q}$ and $\ddot{q}$	vectors of joint position, velocity and acceleration of robot	$\varepsilon$	positive number
		$\rho$	parametric uncertainty



## References

- Bailey, E. and Arapostathis A., "Simple Sliding Mode Control Scheme Applied to Robot Manipulators", *Int. J. Control.*, 45, 4, 1197-1209, 1987.
- Corless, M. and Leitmann, G. "Continuous State Feedback Guaranteeing Uniform Ultimate Boundedness for Uncertain Dynamics Systems", *IEEE T. Automat. Cont.*, A-C-26, 1139-1144, 1981.
- Chen, Y.F., Mita, T. and Wakui, S., "A New Simple Algorithm for Sliding Mode Control of the Robot Arm", *IEEE T. Automat. Cont.*, 35, 828-829, 1990.
- Chen, C. and Xu, R., "Tracking Control of Robot Manipulator Using Sliding Mode Controller with Performance Robustness", *J. Dyn. Syst.-T. ASME*, 121, 64-70, 1999.
- Egeland, O. and Godhavn, J.-M., "A Note on Lyapunov Stability for Adaptive Robot Control", *IEEE T. Automat. Cont.*, 39, 8, 1671-1673, 1994.
- Ghorbel, F., Fitzmorris, A. and Spong, M.W., "Robustness of Adaptive Control of Robots: Theory and Experiment", *Workshop Nonlinear Adaptive Control Issues Robot*, Grenoble, France, Nov. 21-23, 1990.
- Koivo, A.J., "Fundamentals for Control of Robotics Manipulators", John Wiley and Sons, Inc. New York, 1989.
- Koo, K.M. and Kim, J.H., "Robust Control of Robot Manipulators with Parametric Uncertainty", *IEEE T. Automat. Cont.*, 39, 6, 1230-1233, 1994.
- Leitmann, G., "On the Efficiency of Nonlinear Control in Uncertain Linear System", *J. Dyn. Meas. Contr.*, 102, 95-102, 1981.
- Sciavicco, L. and Siciliano, B., "Modeling and Control of Robot Manipulator", McGraw-Hill, New York, 1996.
- Slotine, J.J.E., "The Robust Control of Robot Manipulators", *Int. J. Robot. Res.*, 4, 49-63, 1985.
- Slotine, J.J.E. and Li, W., "On the Adaptive Control of Robotic Manipulators", *Int. J. Robot. Res.*, 6, 49-59, 1987.
- Slotine, J.J.E. and Li, W., "Adaptive Manipulator Control: A Case Study", *IEEE T. Automat. Cont.*, 33, 11, 994-1003, 1988.
- Slotine, J.J.E. and Sastry, S. S., "Tracking Control of Non-Linear System Using Sliding Surface with Application to Robot Manipulators", *Int. J. Control.*, 38, 465-492, 1983.
- Spong, M.W., "On the Robust Control of Robot Manipulators", *IEEE T. Automat. Cont.*, 37, 1782-1786, 1992.
- Spong, M.W., Ortega, R. and Kelley, R., "Comment on Adaptive Manipulator Control: A Case Study", *IEEE T. Automat. Cont.*, 35, 761-762, 1990.
- Spong, M.W. and Vidyasagar, M., "Robot Dynamics and Control", Wiley, New York, 1989.
- Spong, M.W. and Vidyasagar, M., "Robust Linear Compensator Design for Nonlinear Robotic Control", *IEEE T. Robot. Autom.*, 3, 345-350, 1987.
- Rivin, E.I., "Mechanical Design of Robots", McGraw-Hill, New York, 1987.
- Yaz, E., "Comments on the Robust Control of Robot Manipulators", *IEEE T. on Automat. Cont.*, 38, 511-512, 1993.
- Yeung, K.S. and Chen, Y.P., "A New Controller Design for Manipulators Using the Theory of Variable Structure Systems", *IEEE T. Automat. Cont.*, 33, 200-206, 1988.
- Young, K.D., "Controller Design for a Manipulator Using Theory of Variable Structure Systems", *IEEE Trans. Sys. Man. Cybern.*, SMC-8, 101-109, 1978.